Copy 255

RM A52K14

RESEARCH MEMORANDUM

EXPERIMENTAL INVESTIGATION OF THE AERODYNAMIC CHARACTERISTICS OF AN AIR-TO-AIR MISSILE EMPLOYING CRUCIFORM WINGS AND TAIL OF RECTANGULAR PLAN FORM AT MACH NUMBERS OF 1.4 AND 1.9

By Merrill H. Mead

Ames Aeronautical Laboratory
Moffett Field, Calif.

NATIONAL ADVISORY COMMITTEE
FOR AERONAUTICS

WASHINGTON

February 16, 1953

[redacted]

[redacted]

NATIONAL ADVISORY COMMITTEE FOR AERONAUTICS

RESEARCH MEMORANDUM

EXPERIMENTAL INVESTIGATION OF THE AERODYNAMIC CHARACTERISTICS OF AN AIR-TO-AIR MISSILE EMPLOYING CRUCIFORM WINGS AND TAIL OF RECTANGULAR PLAN FORM AT MACH NUMBERS OF 1.4 AND 1.9

By Merrill H. Mead

SUMMARY

The aerodynamic characteristics of a model of an air-to-air missile employing variable-incidence cruciform wings of rectangular plan form and a fixed cruciform tail of rectangular plan form, and the characteristics of its body-wing and body-tail components, as determined from a wind-tunnel investigation for Mach numbers of 1.4 and 1.9, are presented. The results include normal-force, pitching-moment, and axial-force data for the body-wing-tail, body-wing, and body-tail combinations, and normal-force, hinge-moment, and axial-force data for the individual wing panels. The investigation was conducted at a constant Reynolds number of 1.51 million based on the wing chord. All the results are presented in coefficient form plotted against angle of attack. No discussion of the results is included.

INTRODUCTION

One of the most promising defenses against the high-altitude, high-speed bomber is the air-to-air guided missile. The need for developing accurate and reliable guided missiles becomes increasingly important as continuing advancements are made in the performance of bomber- and attack-type aircraft. The problems associated with the aerodynamic design of air-to-air missiles are often complicated by physical restrictions placed upon the size and shape of the missile and its various components to facilitate its stowage aboard small fighter or interceptor aircraft. Paramount among these restrictions is usually a limitation on the span of the lifting surfaces. To reconcile the high-normal-acceleration performance generally required of an air-to-air missile with the desirability of small-span lifting surfaces becomes one of the major problems facing the missile designer. One approach to a solution to this problem

[redacted]

[redacted]

lies in the use of low-aspect-ratio rectangular lifting surfaces. The present report presents the results of a wind-tunnel investigation of the aerodynamic characteristics at Mach numbers of 1.4 to 1.9 of one such missile configuration. In order to expedite publication of these data, no analyses or applications of the data are included in the present report.

NOTATION

c wing chord, feet

C_{h_w} wing-hinge-moment coefficient (based on the exposed area of one wing panel[1] and the wing chord) $\left(\frac{\text{wing hinge moment}}{qS_1c}\right)$

C_m pitching-moment coefficient about the model center of gravity (based on the exposed area of two wing panels and the wing chord) $\left(\frac{\text{pitching moment}}{qSc}\right)$

C_X axial-force coefficient (force measured parallel to body longitudinal axis, based on the exposed area of two wing panels) $\left(\frac{\text{axial force}}{qS}\right)$

C_{X_w} wing-axial-force coefficient (component of force on one wing panel parallel to body longitudinal axis, based on the exposed area of one wing panel) $\left(\frac{\text{wing axial force}}{qS_1}\right)$

C_Z normal-force coefficient (force measured normal to body longitudinal axis, based on the exposed area of two wing panels) $\left(\frac{\text{normal force}}{qS}\right)$

C_{Z_w} wing-normal-force coefficient (component of force on one wing panel normal to body longitudinal axis, based on the exposed area of one wing panel) $\left(\frac{\text{wing normal force}}{qS_1}\right)$

[1] As used in this report, the complete cruciform wing is composed of four wing panels.

M	Mach number
q	dynamic pressure, pounds per square foot
R	Reynolds number
S	exposed area of two wing panels, square feet
S_1	exposed area of one wing panel, square feet
α	angle of attack of body center line, degrees
δ	angle of incidence of wing panel (angle between the wing chord and the body longitudinal axis), degrees
φ	angle of bank, degrees

The directions of positive forces, moments, and angles are indicated in the sketch of figure 1.

APPARATUS

The investigation was conducted in the Ames 6- by 6-foot supersonic wind tunnel at Mach numbers of 1.4 and 1.9. This wind tunnel is a closed-return, variable-pressure supersonic wind tunnel in which the Mach number can be varied continuously from 0.60 to 0.93 and from 1.15 to 1.9. The wind tunnel and its stream characteristics are described in detail in reference 1.

MODEL AND SUPPORT

The model investigated (fig. 2) consisted of two sets of cruciform lifting surfaces mounted on a pointed, cylindrical body having a fineness ratio of 16. The forward (wing) surfaces were of rectangular plan form with an aspect ratio of 1.16 based on the exposed area and span (excluding the body) of two wing panels. The wing panels were composed of symmetrical, double-wedge sections with a maximum thickness of 3 percent at 50 percent of the wing chord. Each panel was movable and was hinged at the 50-percent-chord station. With the wings at zero incidence, the gap between the inner edge of each wing and the body was approximately 0.016-inch, or about 1/10 percent of the wing span.

The rear (tail) surfaces were also of rectangular plan form and had an aspect ratio of 0.48. The tail panels were fixed rigidly to the body

[redacted]

and were constructed of 0.25-inch flat plate with leading and trailing edges rounded. Provision was made in the design of the model for testing various combinations of the model components separately. The model could therefore be assembled as a body-wing-tail combination, a body-wing combination, or a body-tail combination.

All components of the model were constructed of steel, with the exception of the detachable, ogive nose section of the body which was of aluminum.

The model was mounted in the wind tunnel on a cantilever-beam-type support sting. The downstream end of the support sting was pin connected to two cross-stream supporting members. Differential movement of the two cross-stream members pitched the model in the horizontal plane of the wind tunnel without changing its relative position in the tunnel. A bent support sting was employed in order to obtain an angle-of-attack range of from -8° to $+20^\circ$.

MEASUREMENTS AND CORRECTIONS

The normal forces, axial forces, and pitching moments on the model were measured by means of a four-component[2] electrical strain-gage balance contained within the body of the model. The electrical unbalance of each strain gage, under an applied load, was measured by a recording light-beam galvanometer.

Flexure-type, X-beam balances mounted within the body of the model at each wing-body juncture (see fig. 2) measured the normal forces, axial forces, and hinge moments on each individual wing panel. The general arrangement of the X-beam balance is shown in figure 3. In operation, the wing panel is mounted rigidly on the wing mounting block, shown in the sketch, by means of a short connecting shaft. The load applied to the wing is transferred through the wing mounting block and beam flexures to the bending beams. The applied load is then resolved into four force vectors parallel to the four bending beams and the magnitudes of the force vectors are measured by means of electrical strain gages mounted on each bending beam. Since the system can be assumed to represent a pin-connected, pin-loaded truss, the four measured force components can

[2]Although the rolling-moment component of the balance was operative during the investigation, these data are not presented since, with the exception of one series of tests, conditions of symmetry existed which produced no rolling moments on the model. During the tests of the body-wing combination, in which the model was pitched through the angle-of-attack range at various preset angles of bank, small rolling moments were recorded but these were within the limits of precision of the rolling-moment component of the balance and are therefore not presented.

[redacted]

then be resolved into two forces, normal and parallel to the body longitudinal axis, and a moment about the hinge line. The components of the applied load tending to produce side force, yawing moment, and rolling moment on the wing are transferred through the wing mounting block and suitable restraint flexures to the model body structure and are not measured.

The four-component balance and the X-beam balances were calibrated in the wind tunnel periodically throughout the investigation by applying known forces and moments to the model.

The sketch of the model presented in figure 1 indicates the direction of positive forces, moments, and angles according to the sign convention followed in this investigation. It should be pointed out, however, that for the tests of the model in a banked attitude, the model was rolled about the four-component balance, which remained fixed. Under these conditions, the normal force measured by the four-component balance was in every case the component in the plane in which the model angle of attack was varied, regardless of the angle of bank. Likewise the measured pitching moment was always the component of pitching moment about an axis through the center of gravity of the model normal to the plane in which the model angle of attack was varied. The wing normal force measured by the X-beam balances, on the other hand, was always the component of normal force on the wing acting normal to the plane through the hinge line and the body longitudinal axis. In other words, the directions of the wing-normal-force vectors changed with both angles of attack and bank, while the direction of the total normal-force vector (measured by the four-component balance) changed with angle of attack but was invariant with angle of bank. Note that when the wings were set at an angle of incidence with respect to the body, this arrangement resulted in measured wing normal forces which were normal not to the wing-chord plane, but always to the plane passing through the hinge line and the body longitudinal axis.

The effects of small stream irregularities, known to exist in the Ames 6- by 6-foot supersonic wind tunnel (reference 1), on the measured aerodynamic characteristics have been minimized in the present investigation by varying the model incidence in the horizontal plane of the wind tunnel, thereby utilizing the most favorable flow conditions. This procedure limited the adverse effects of stream irregularities to the axial buoyancy effect on the model resulting from a longitudinal pressure gradient in the wind tunnel, and a small effective angle of yaw resulting from the flow angularity in the vertical plane of the wind tunnel (model yaw plane). The measured axial forces were corrected for this buoyancy effect by utilizing the stream-survey data presented in reference 1. The pressure at the base of the model was measured throughout the investigation by means of a liquid manometer connected to three pressure orifices at the model base. The measured axial forces were then adjusted to

[redacted]

correspond to free-stream static pressure acting on the base. The flow deviations in the vertical plane of the wind tunnel had a negligible effect on the forces and moments measured by the four-component balance, since this effect would have manifested itself primarily as changes in the side-force, yawing-moment, and rolling-moment characteristics of the model. However, the effect of this small angle of yaw was observed in the wing normal forces and hinge moments measured by the X-beam balances for the two vertical wings[3] at zero bank angle, and for all four wings to a lesser extent when the model was in a banked attitude. No corrections have been applied to the data for this effect.

The angles of attack presented in the plotted data have been corrected for deflection of the model under load with data obtained from deflection calibrations of the model, balance, and support system prior to the wind-tunnel tests.

Deflection calibrations of the variable-incidence wings indicated that, for the range of loads imposed on the wings in these wind-tunnel tests, the angular deflections of the wing panels were negligible.

TESTS

The investigation was conducted in three phases which included tests of the body-wing-tail combination, the body-wing combination, and the body-tail combination. Each test was conducted at Mach numbers of 1.4 and 1.9 at a constant Reynolds number of 1.51 million based on the wing chord. The angle-of-attack range was from -8° to $+20^\circ$ in each case except where the strength limitations of the balance reduced the maximum angle. The investigation was conducted as follows:

Body-Wing-Tail Combination

With the model at zero bank angle, normal-force, axial-force, and pitching-moment data were obtained through the angle-of-attack range for angles of horizontal-wing incidence of 0°, 4°, 7°, 10°, and 14°.

Body-Wing Combination

With the model at zero bank angle, normal-force, axial-force, and pitching-moment data, and for the horizontal wings, wing-normal force,

[3]As used in this report, vertical and horizontal wings refer to the components of the cruciform wing which are in the vertical and horizontal planes with the model at zero bank angle in a normal upright attitude and not as mounted in the wind tunnel.

wing-axial-force, and wing-hinge-moment data were obtained through the angle-of-attack range for angles of horizontal-wing incidence of 0°, 4°, 7°, 10°, and 14°.

With the wings at zero incidence, corresponding forces and moments were measured, including wing forces and hinge moments for all four wings, through the angle-of-attack range for angles of bank of 0°, 11-1/4°, 22-1/2°, 33-3/4°, and 45°.

Body-Tail Combination

With the model at zero bank angle, normal-force, axial-force, and pitching-moment data were obtained through the angle-of-attack range.

RESULTS

The data obtained during the investigation have all been reduced to standard NACA coefficient form (as defined under Notation), plotted against corrected angle of attack, and are presented in figures 4 through 9. In order to facilitate publication at the earliest possible date, no discussion or analysis of the results has been included in the present report. Note that the results of each test, as presented below, include the data obtained at both 1.4 and 1.9 Mach numbers and at a Reynolds number of 1.51 million (based on the wing chord), which was held constant throughout the investigation. It should be noted also that in presenting the wing-force and hinge-moment data, the individual wing panels are identified by number according to the convention shown in the sketch of figure 1. With the model in an unbanked attitude, the wing panels are numbered from 1 to 4 beginning with the left horizontal wing panel (looking upstream) and proceeding in a clockwise direction. Each wing panel retains its identifying number as the model is banked.

The normal-force, pitching-moment, and axial-force coefficients for the body-wing-tail combination at zero bank angle are plotted against angle of attack for various angles of horizontal-wing incidence in figures 4(a) and 4(b).

For the body-wing combination, the normal-force, pitching-moment, and axial-force characteristics at zero bank angle and various angles of horizontal-wing incidence are presented in figures 5(a) and 5(b). The variations of wing-normal-force, wing-hinge-moment, and wing-axial-force coefficients with angle of attack, for conditions corresponding to those above, are shown in figures 6(a) through 6(d) for wing panels 1 and 3, the horizontal wing panels of the body-wing combination. The characteristics for both panels should be the same, of course. Both sets of data are presented, however, to illustrate the accuracy of the data. It will

be noted that, in general, the agreement is good for wing normal forces and axial forces, but that the wing hinge moments show considerable disagreement in some cases (i.e., at a Mach number of 1.4).

Presented in figures 7(a) and 7(b) are the normal-force, pitching-moment, and axial-force characteristics for the body-wing combination with the wings at 0° incidence and the model at various angles of bank. The wing-force and hinge-moment coefficients at these test conditions are plotted against angle of attack in figures 8(a) through 8(h) for each of the four wing panels.

Normal-force, pitching-moment, and axial-force coefficients for the body-tail combination are presented in figures 9(a) and 9(b).

Normal-force and pitching-moment data for the body alone have been obtained, for a Mach number of 1.4, during a previous investigation and are presented in reference 2.

Ames Aeronautical Laboratory
National Advisory Committee for Aeronautics
Moffett Field, Calif.

REFERENCES

1. Frick, Charles W., and Olson, Robert N.: Flow Studies in the Asymmetric Adjustable Nozzle of the Ames 6- by 6-Foot Supersonic Wind Tunnel. NACA RM A9E24, 1949.

2. Edwards, S. Sherman: Experimental and Theoretical Study of Factors Influencing the Longitudinal Stability of an Air-to-Air Missile at a Mach Number of 1.4. NACA RM A51J19, 1952.

[redacted]

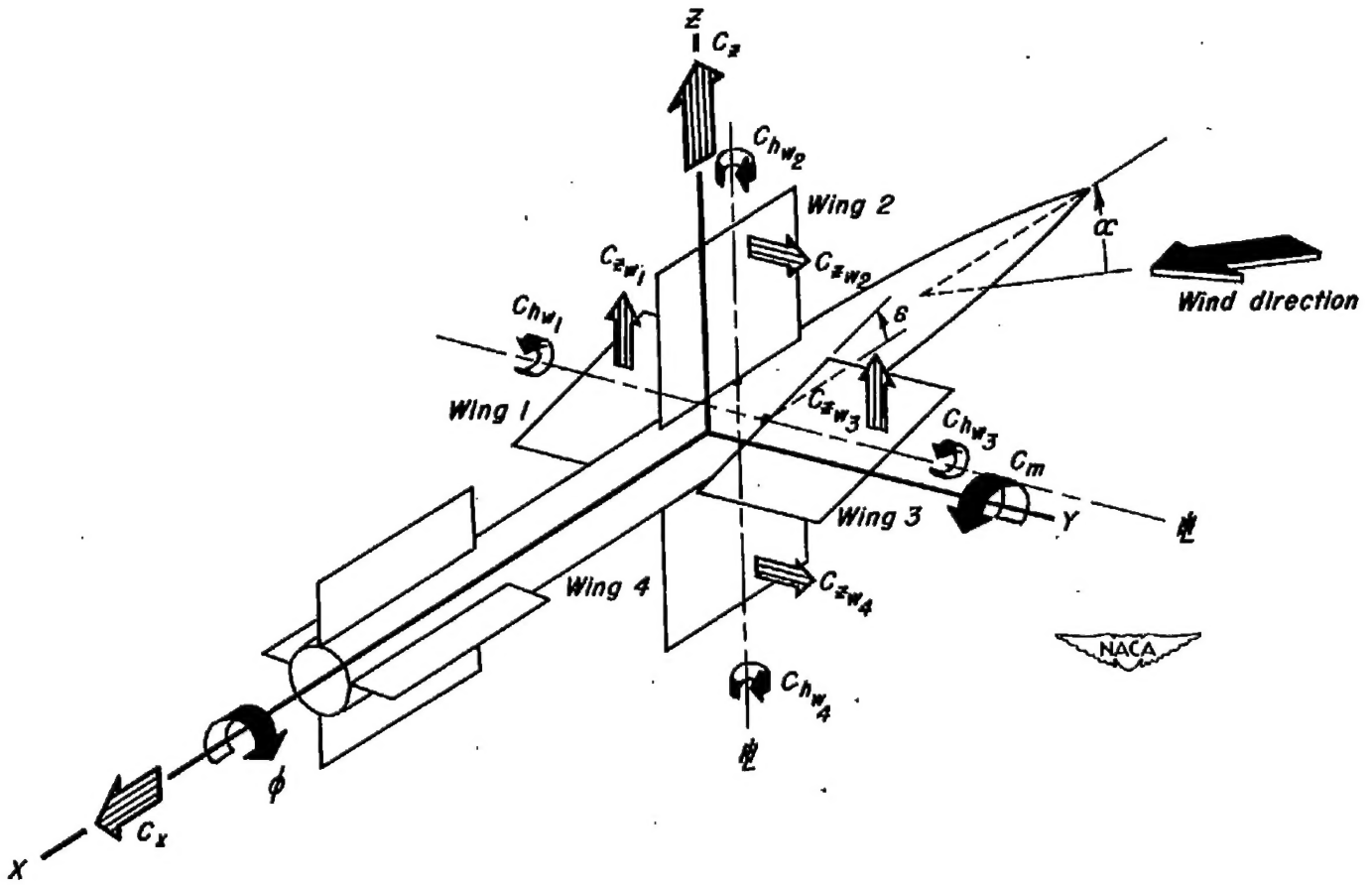

Figure 1.- Sketch of model showing wing-panel identification numbers and directions of positive forces, moments, and angles.

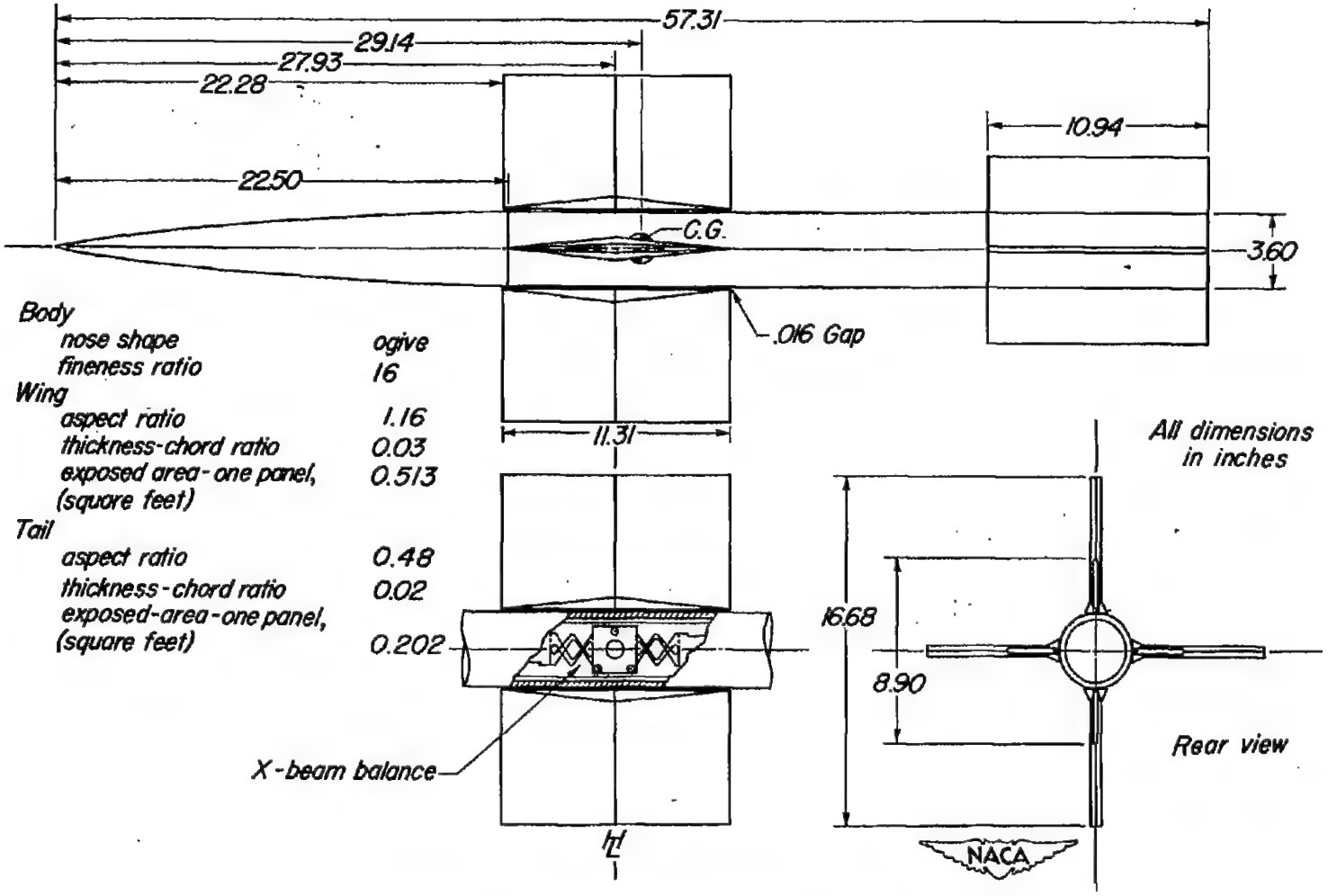

Figure 2.- Geometric characteristics of the model.

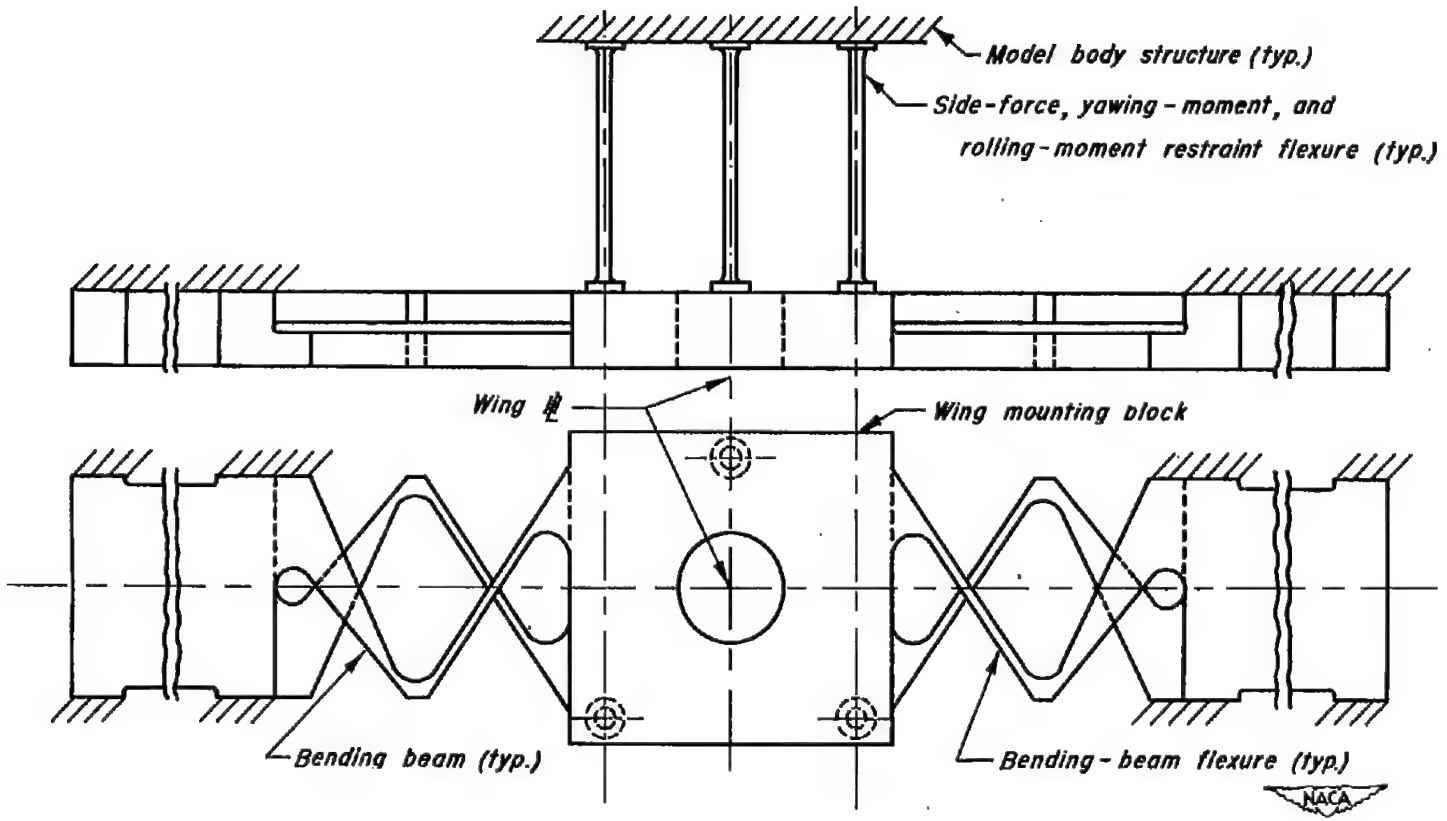

Figure 3.- General arrangement of the X-beam balance.

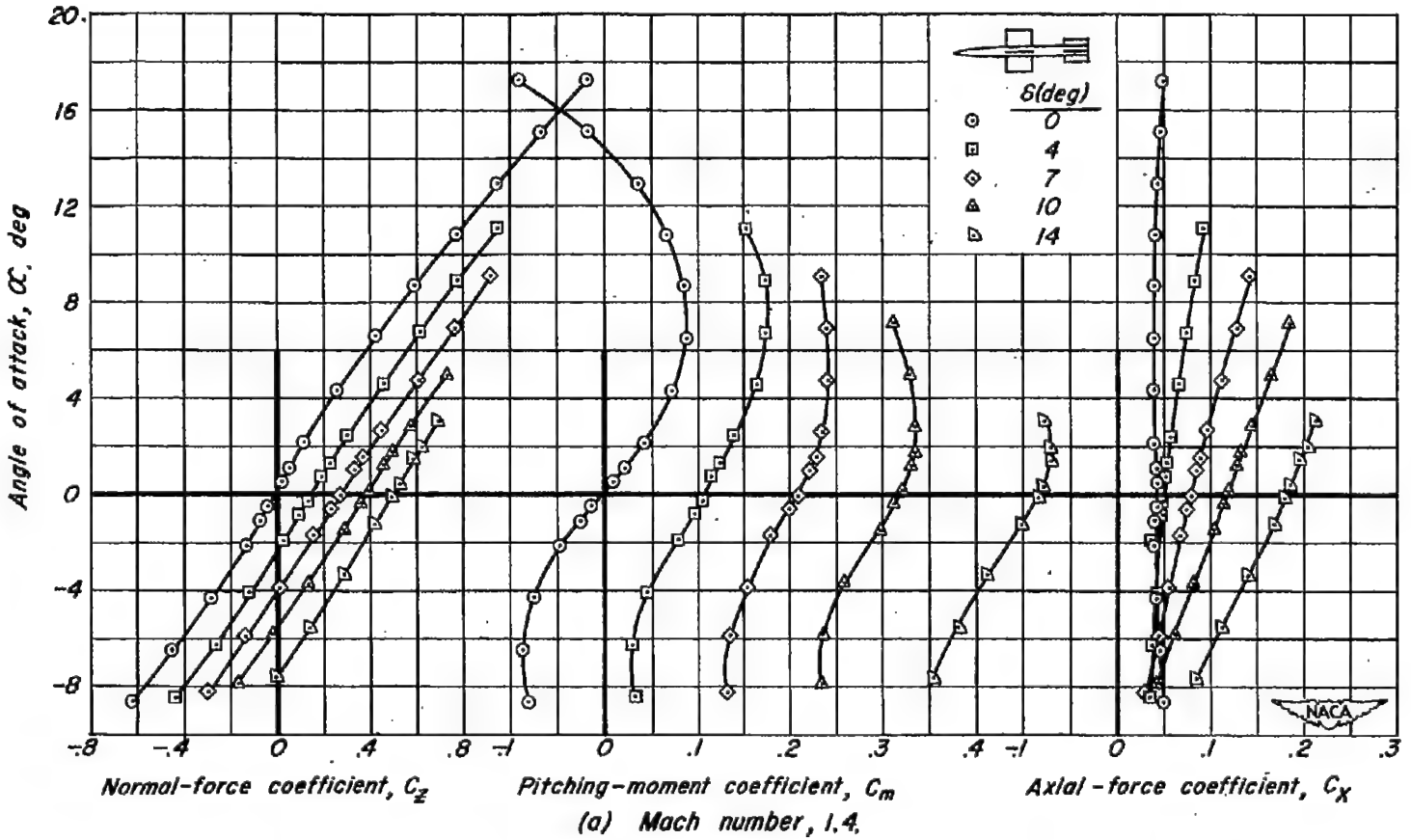

(a) Mach number, 1.4.

Figure 4.- Normal-force, pitching-moment, and axial-force characteristics of the body-wing-tail combinations at 0° bank angle for various angles of horizontal-wing incidence, δ.

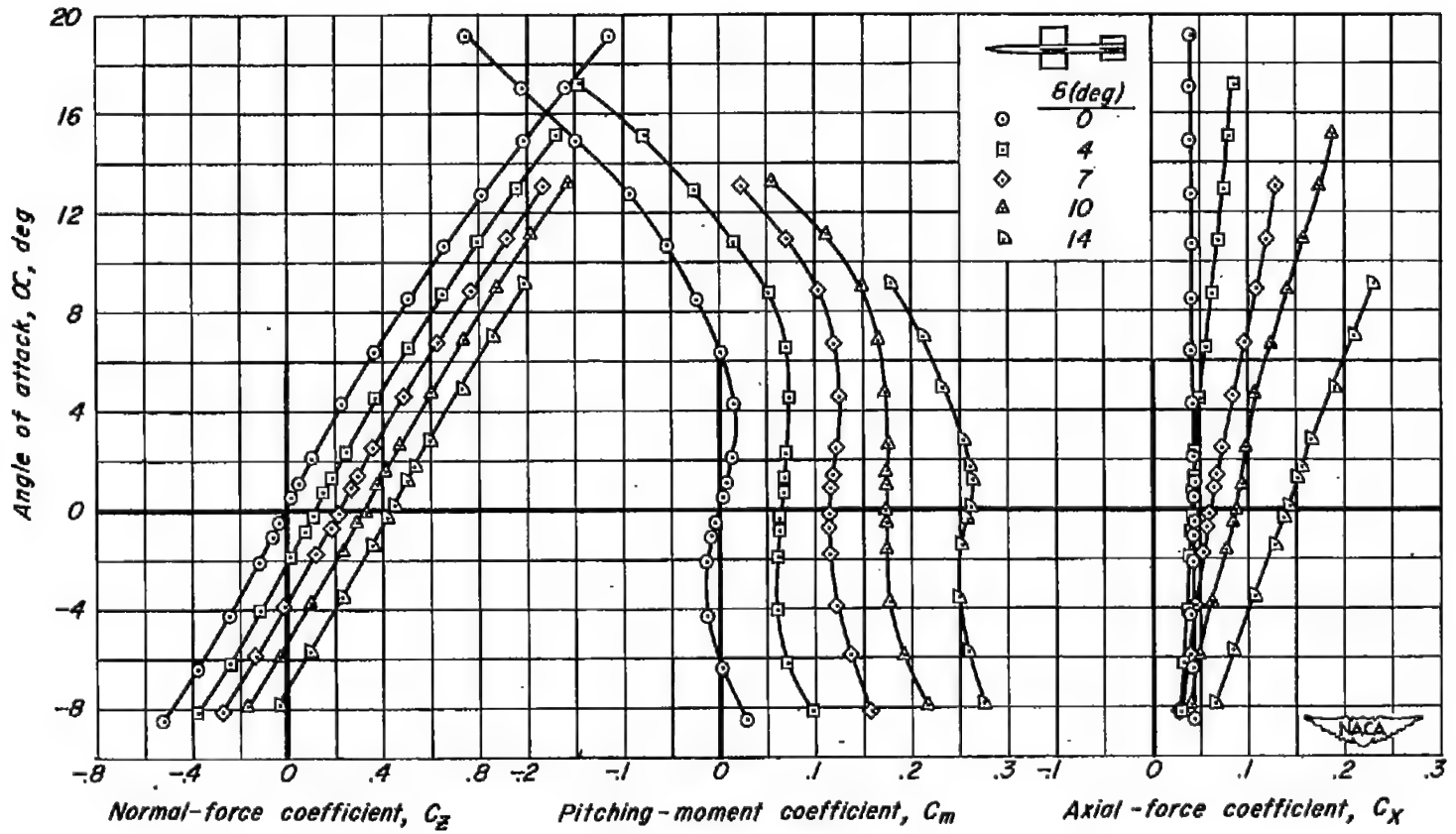

(b) Mach number, 1.9.

Figure 4.- Concluded.

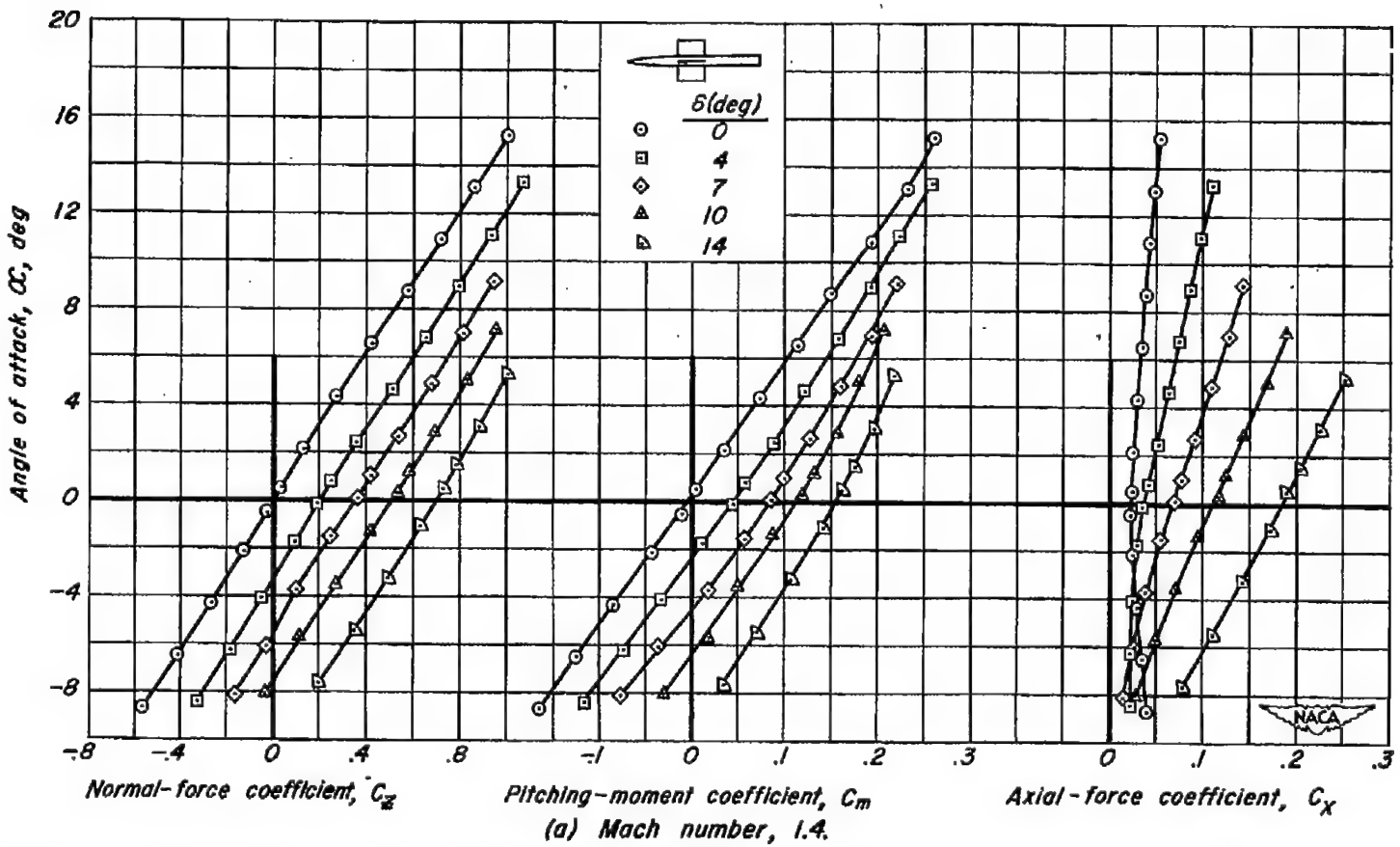

(a) Mach number, 1.4.

Figure 5.- Normal-force, pitching-moment, and axial-force characteristics of the body-wing combination at 0° bank angle for various angles of horizontal-wing incidence, δ.

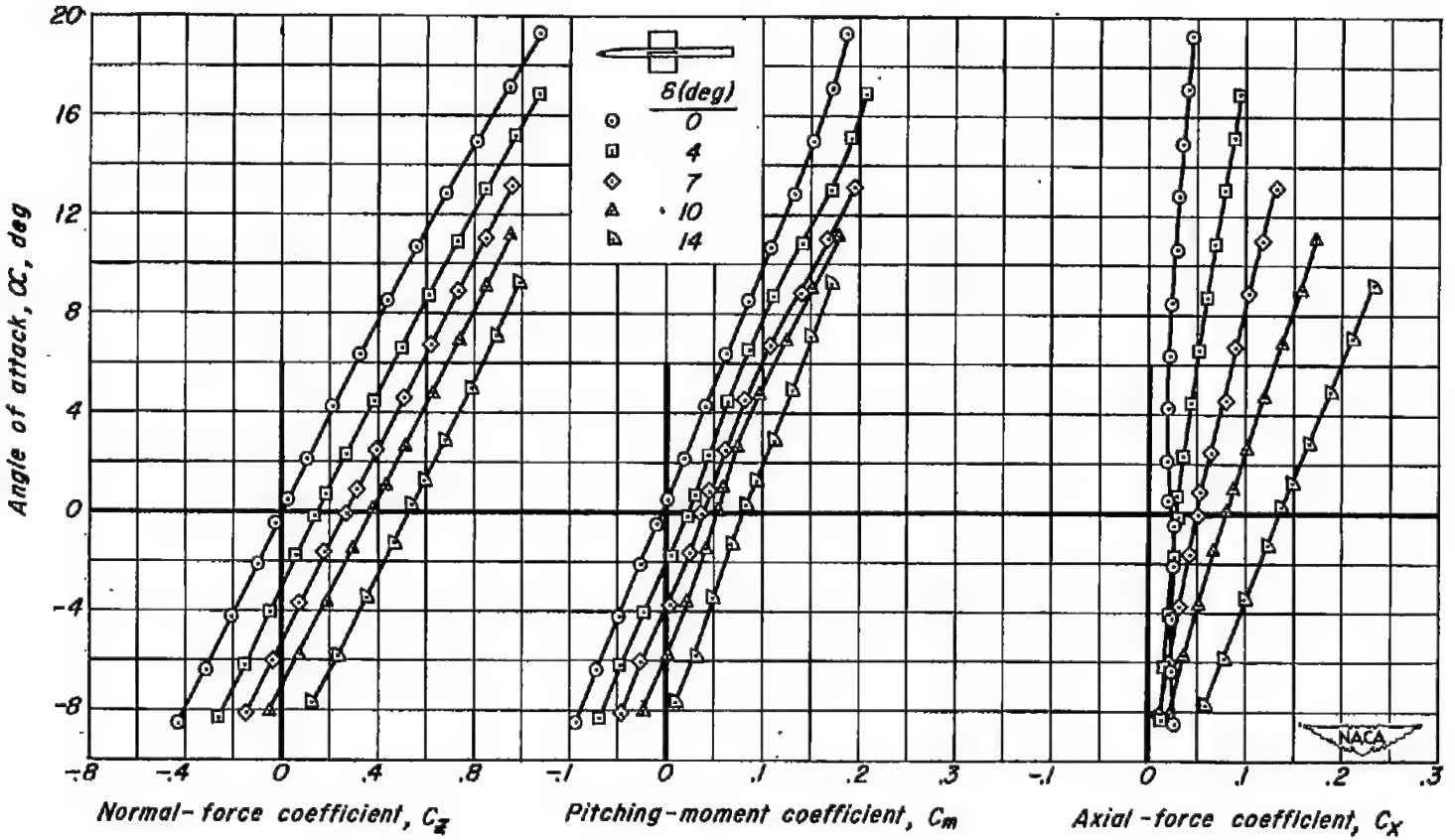

(b) Mach number, 1.9

Figure 5. - Concluded.

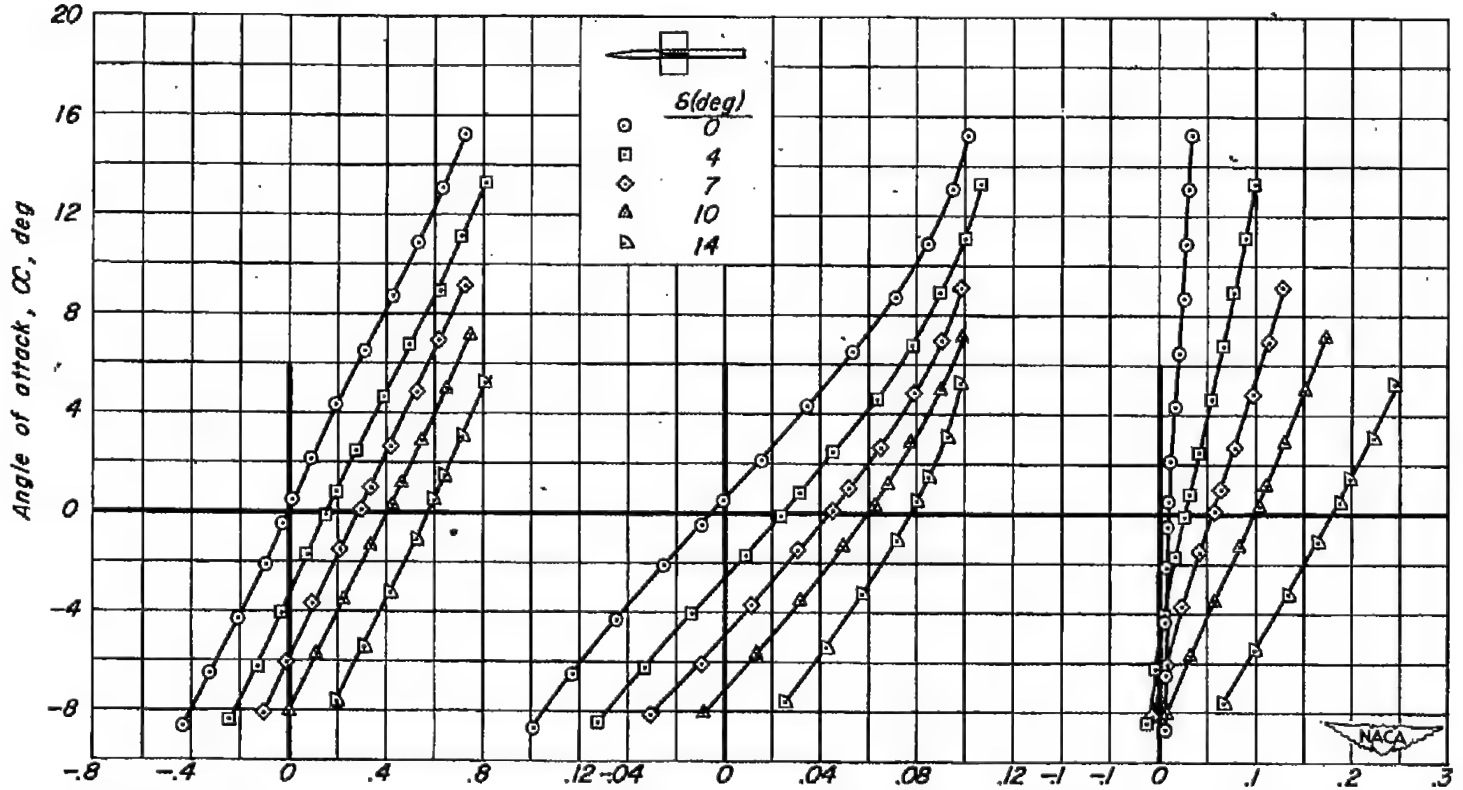

(a) Wing panel 1; Mach number, 1.4.

Figure 6.- Wing-normal-force, hinge-moment, and axial-force characteristics for wing panels 1 and 3 of the body-wing combination at 0° bank angle and various angles of horizontal-wing incidence, δ.

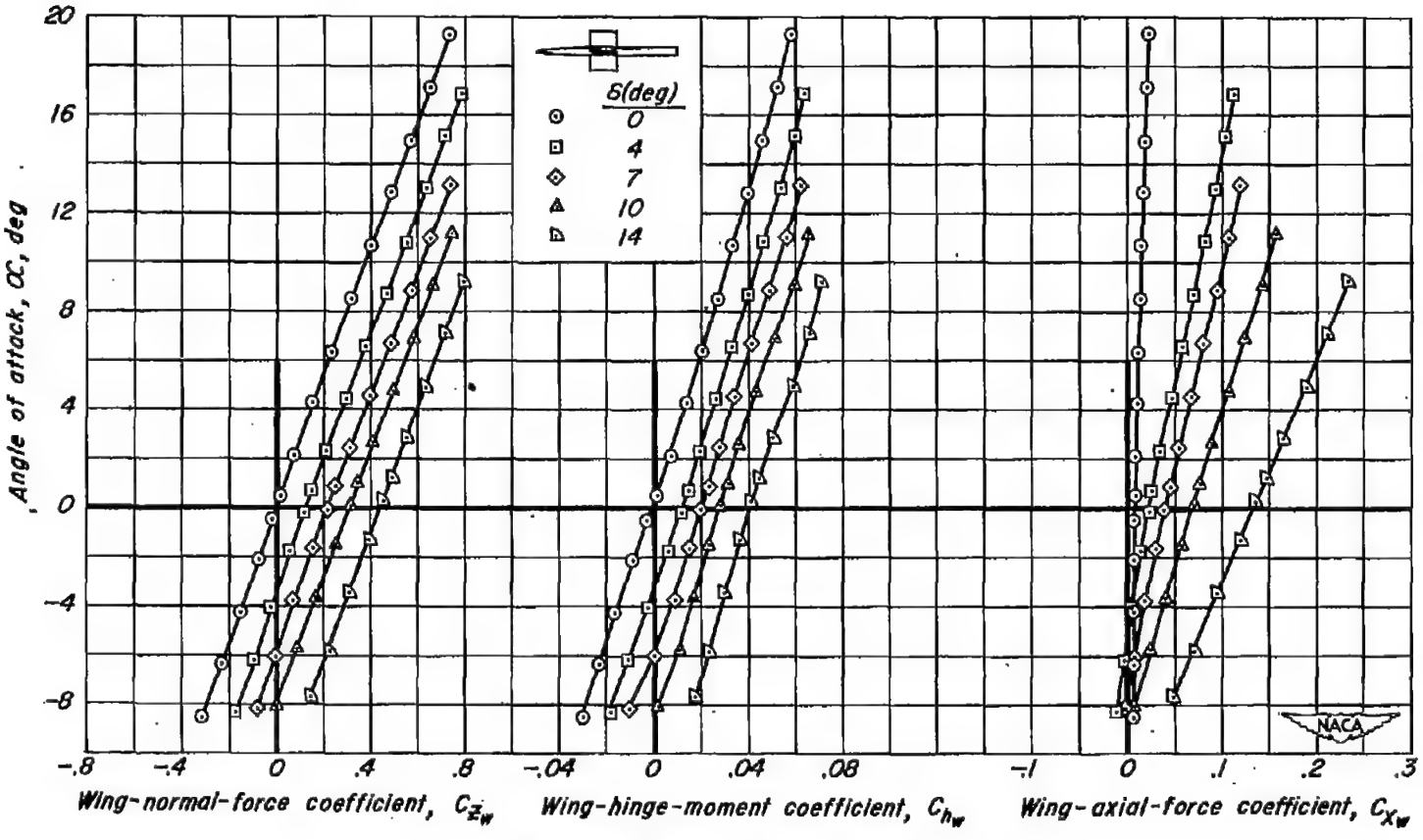

(b) Wing panel 1; Mach number, 1.9.

Figure 6.- Continued.

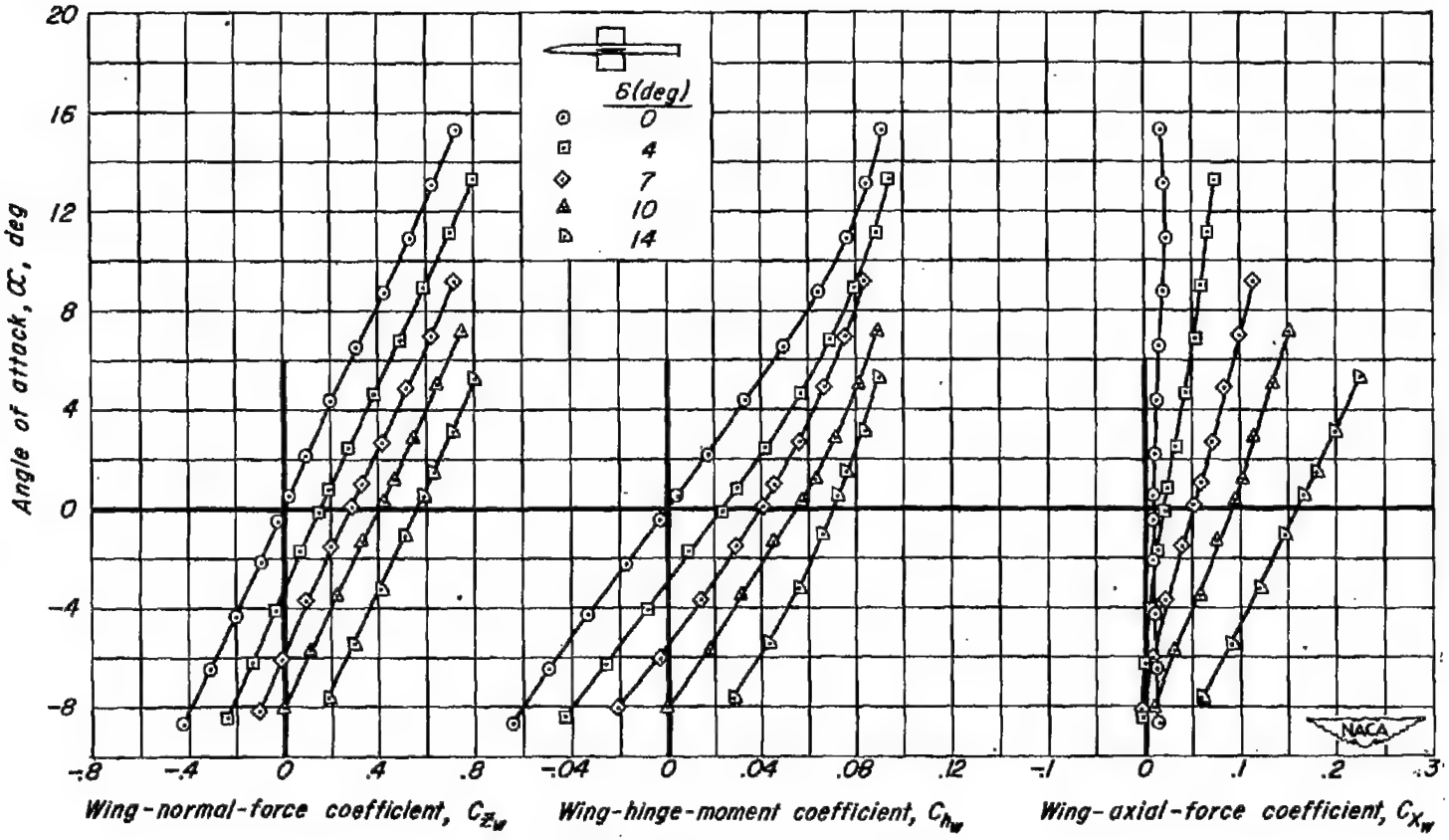

(c) Wing panel 3; Mach number, 1.4.

Figure 6.- Continued.

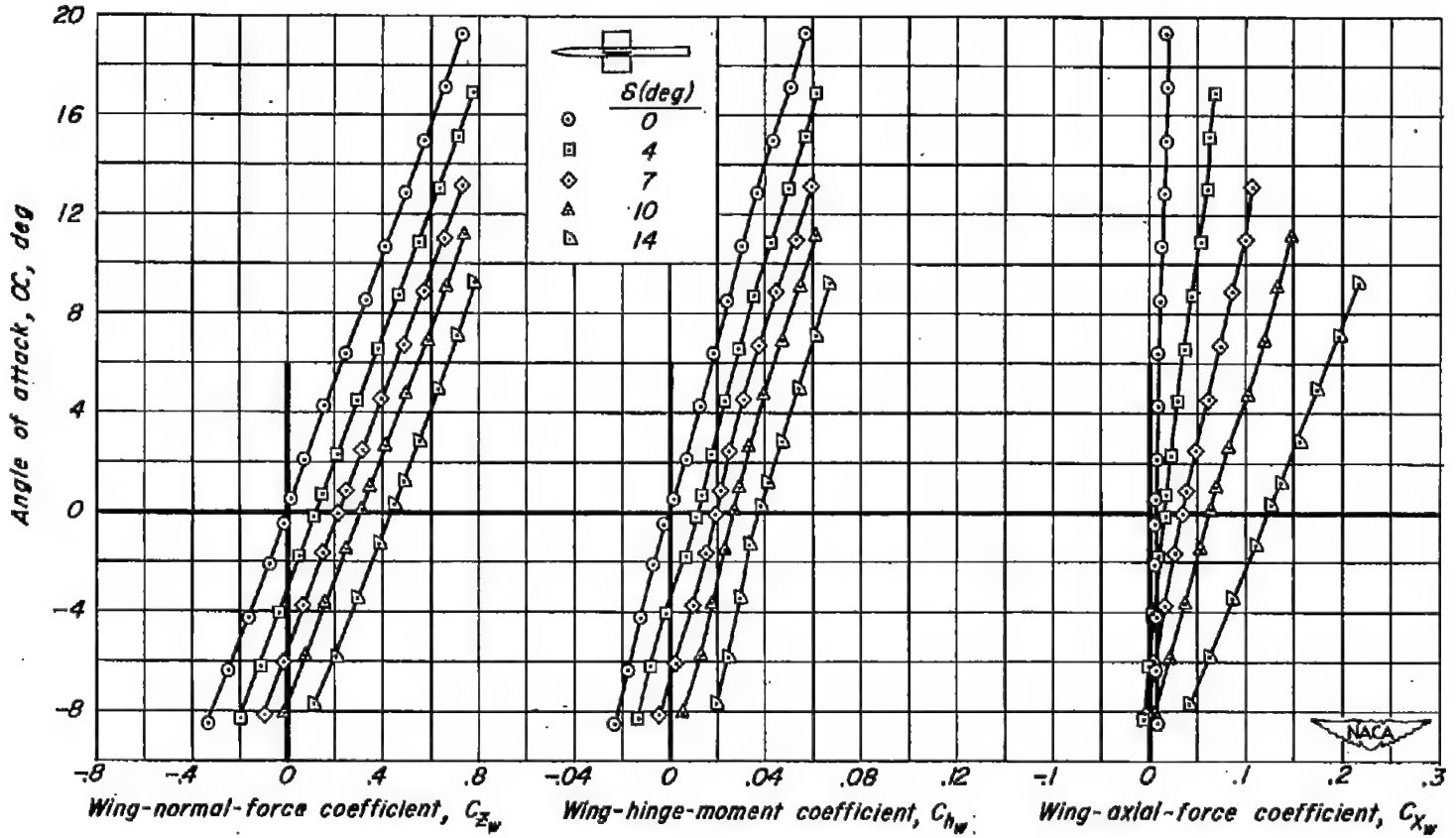

(d) Wing panel 3; Mach number, 1.9.

Figure 6.- Concluded.

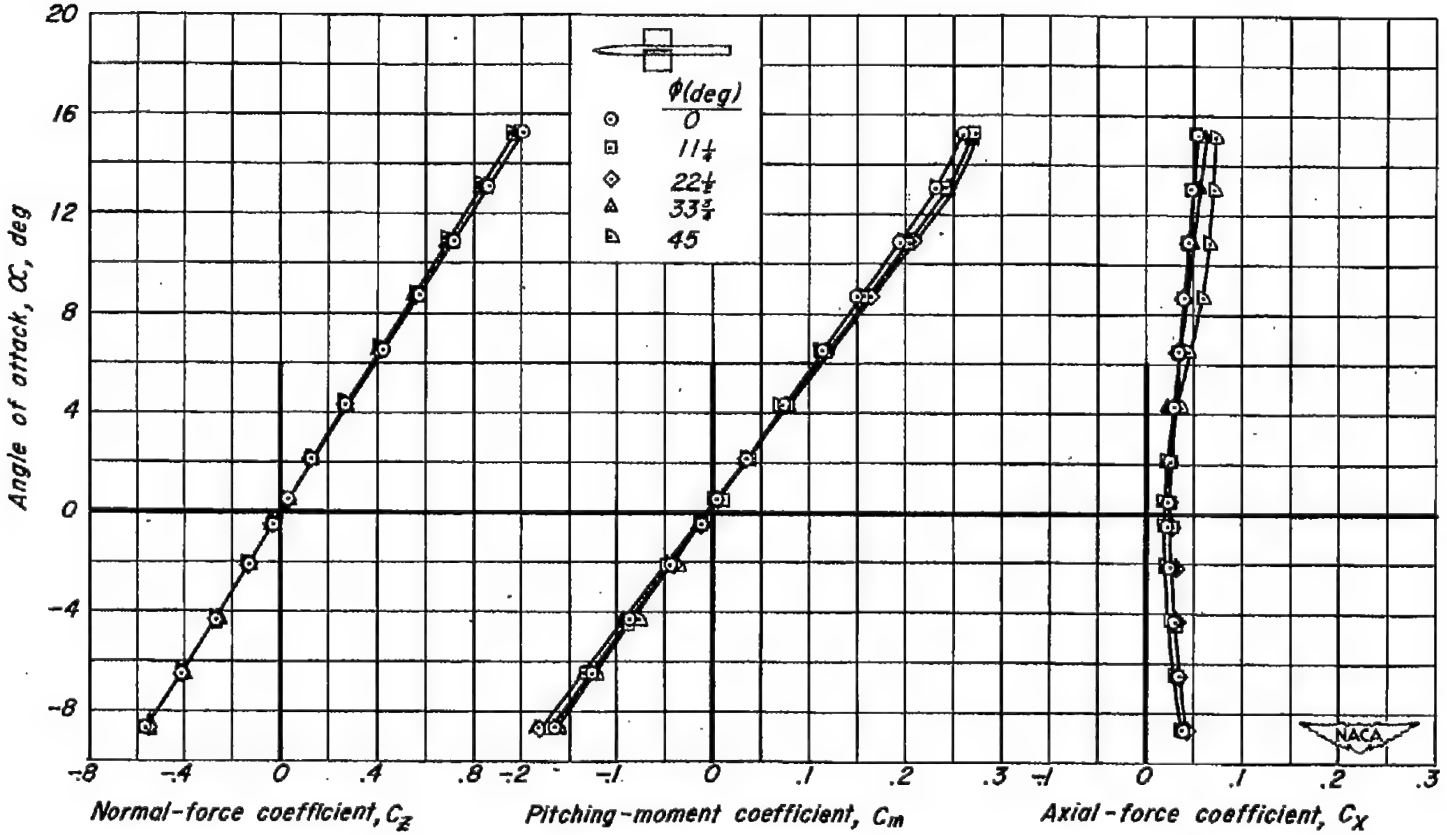

(a) Mach number, 1.4.

Figure 7.- Normal-force, pitching-moment, and axial-force characteristics of the body-wing combination with 0° wing incidence for various angles of bank, φ.

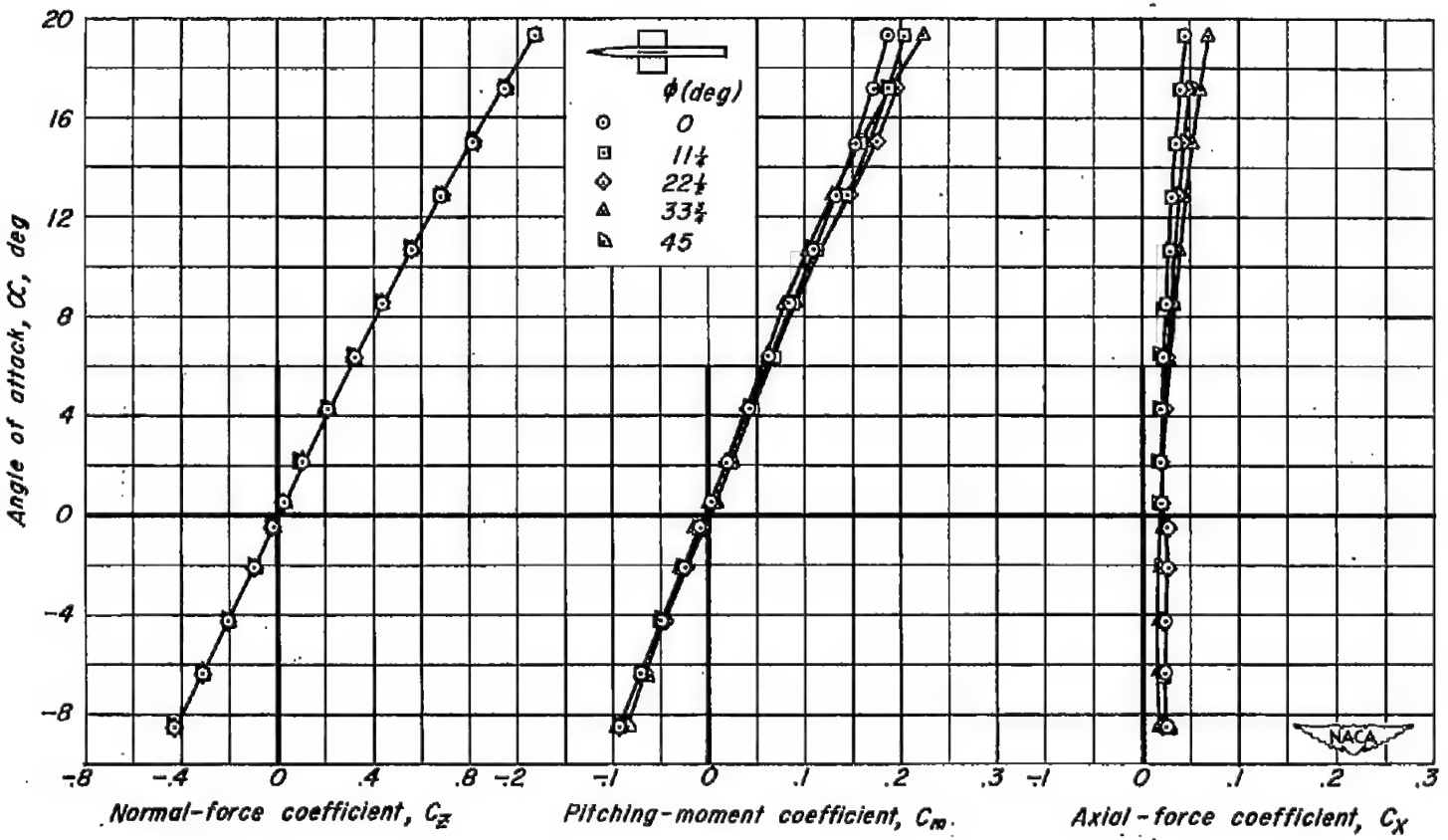

(b) Mach number, 1.9.

Figure 7.- Concluded.

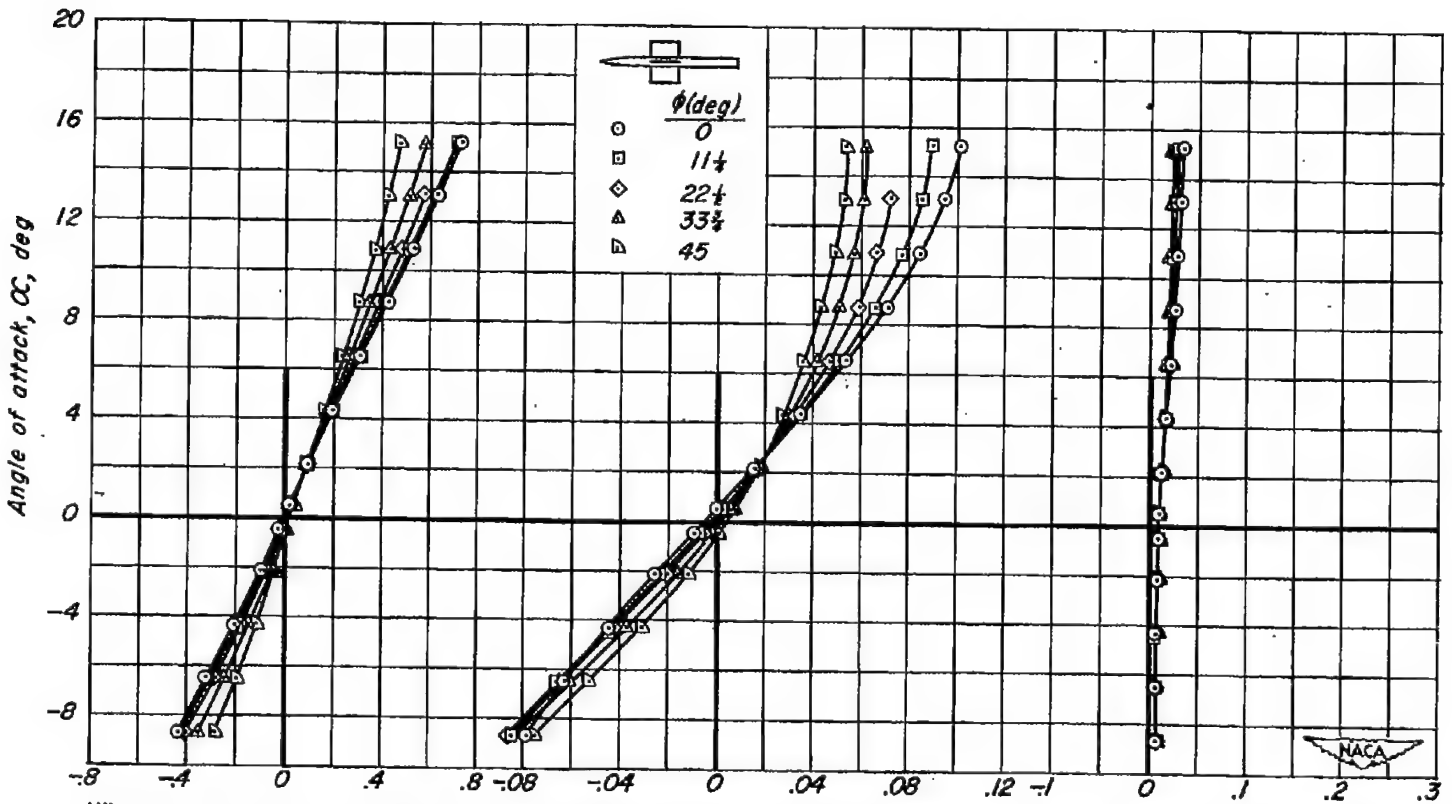

(a) Wing panel 1; Mach number, 1.4.

Figure 8.- Wing-normal-force, hinge-moment, and axial-force characteristics for all wing panels of the body-wing combination with 0° wing incidence at various angles of bank, ϕ.

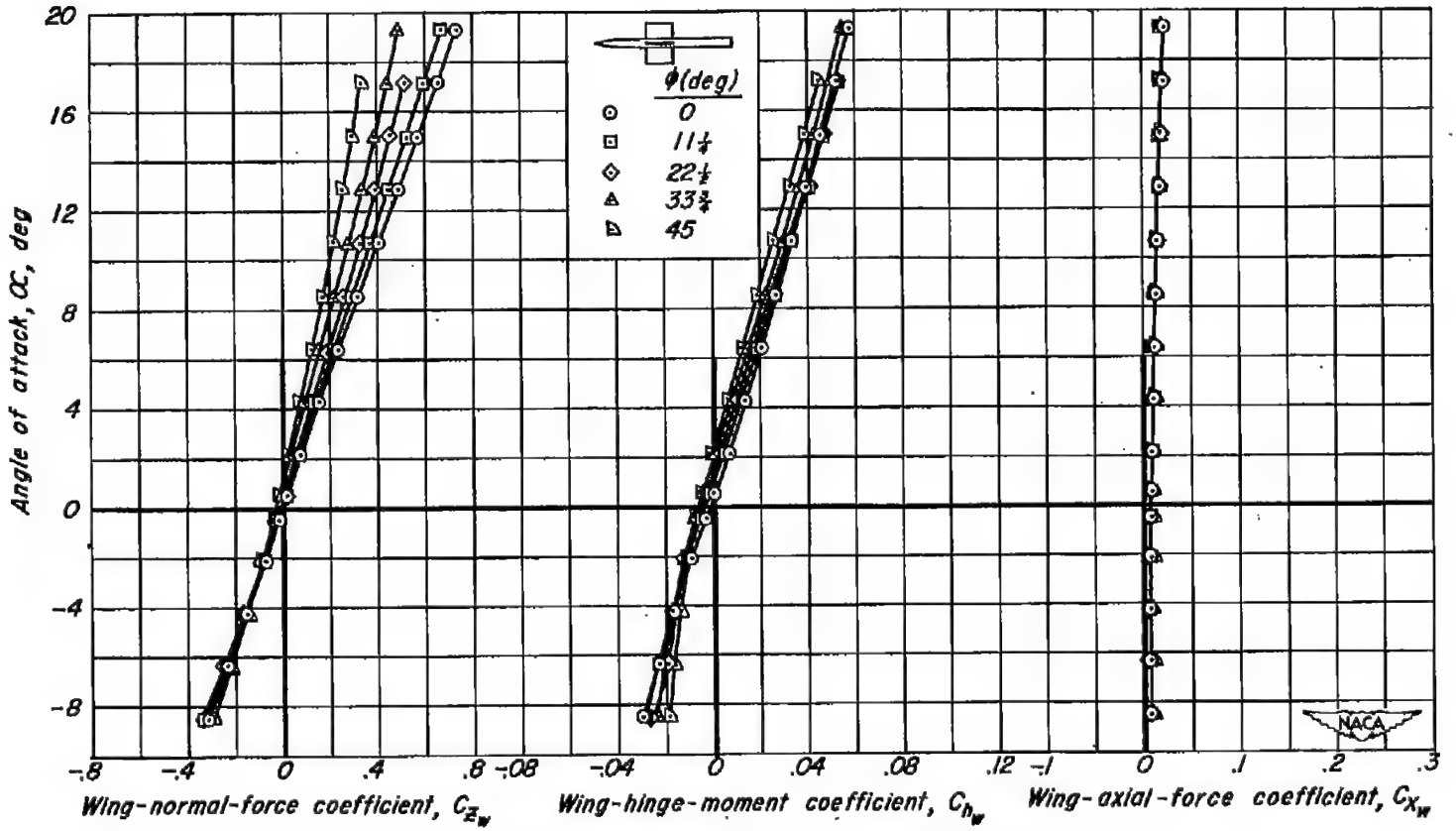

(b) Wing panel 1; Mach number, 1.9.

Figure 8.- Continued.

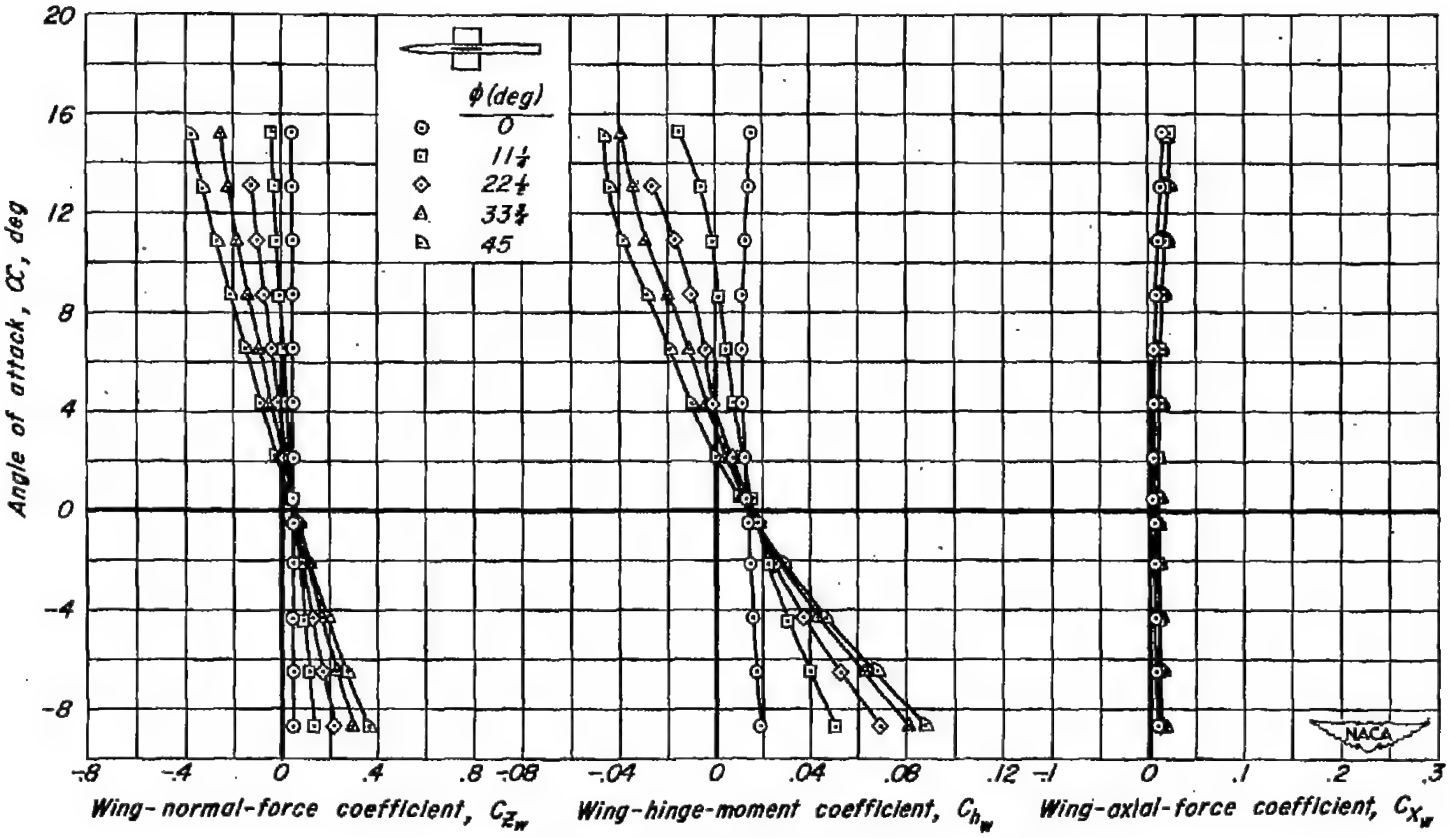

(c) Wing panel 2; Mach number, 1.4.

Figure 8.- Continued.

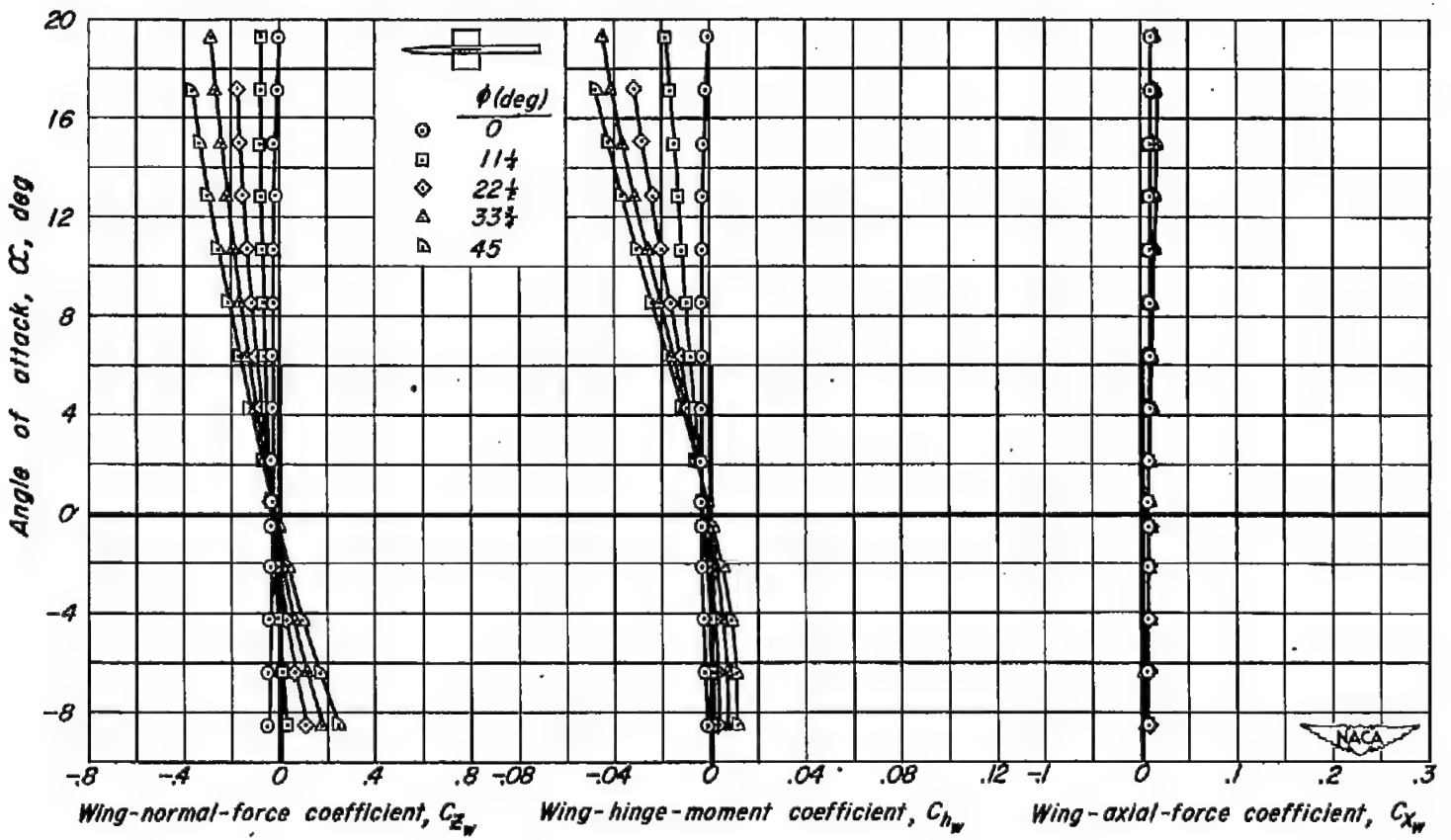

(d) Wing panel 2; Mach number, 1.9.

Figure 8.- Continued.

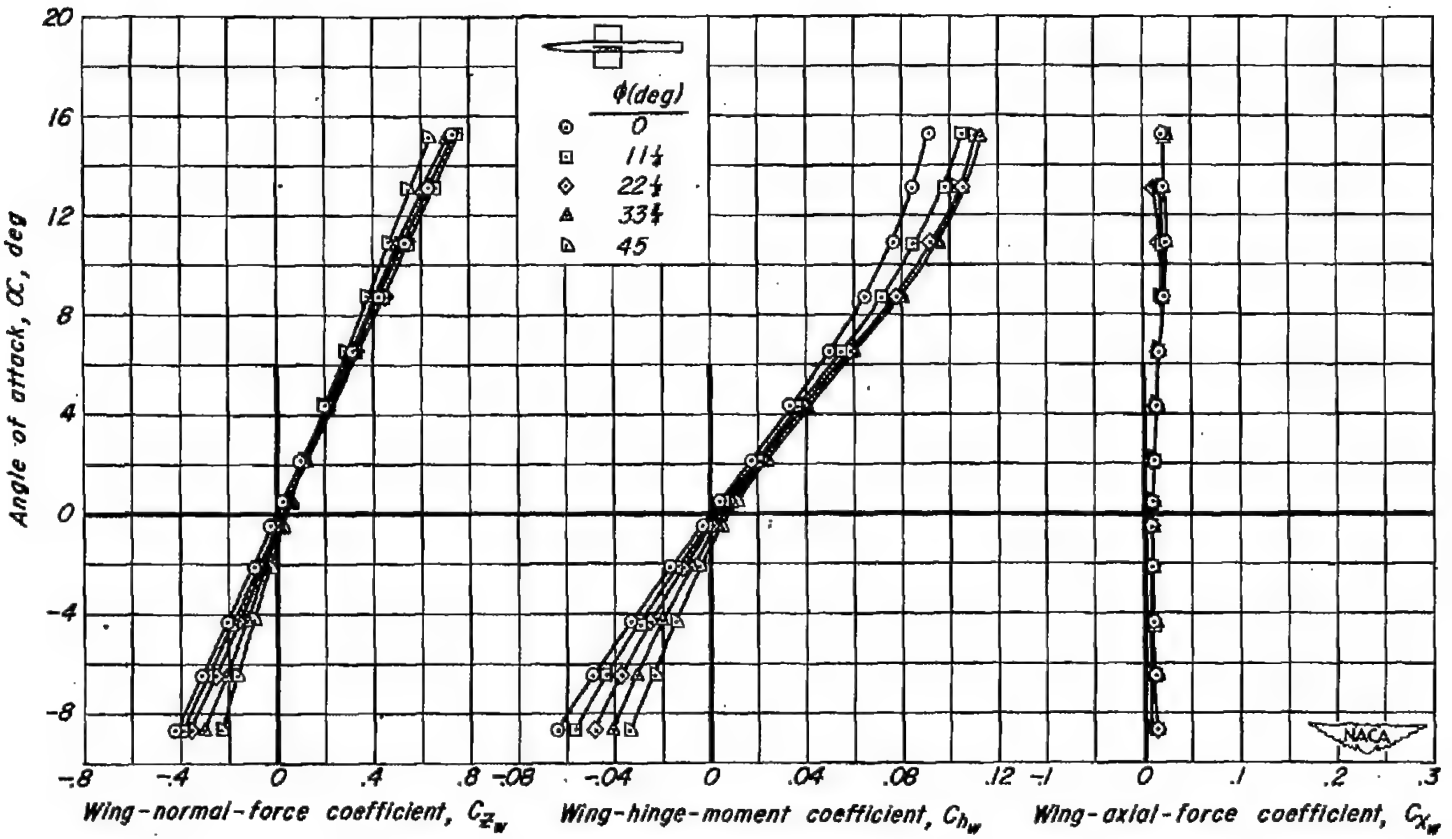

(e) Wing panel 3; Mach number, 1.4.

Figure 8.- Continued.

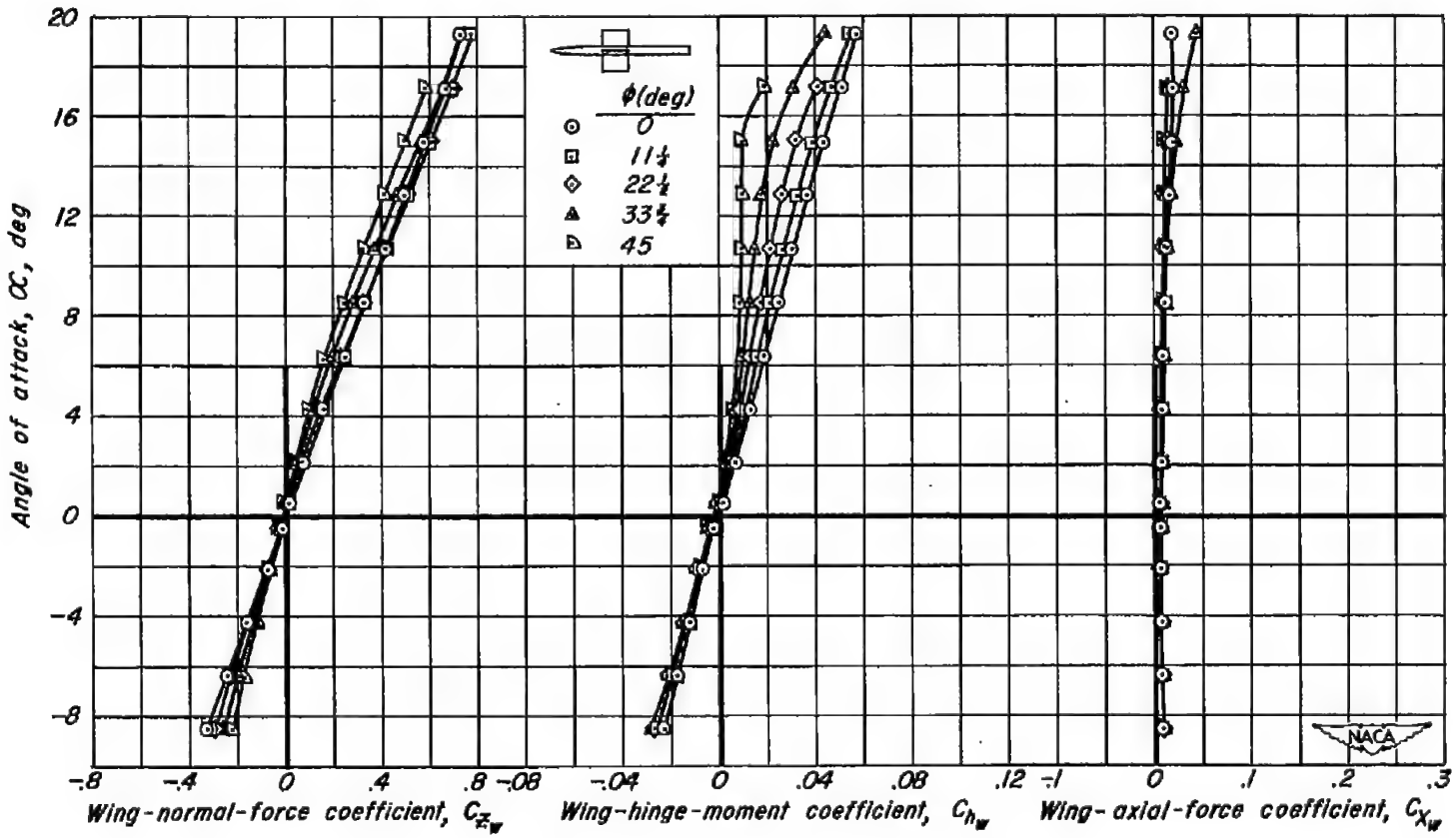

(f) Wing panel 3; Mach number, 1.9.

Figure 8.- Continued.

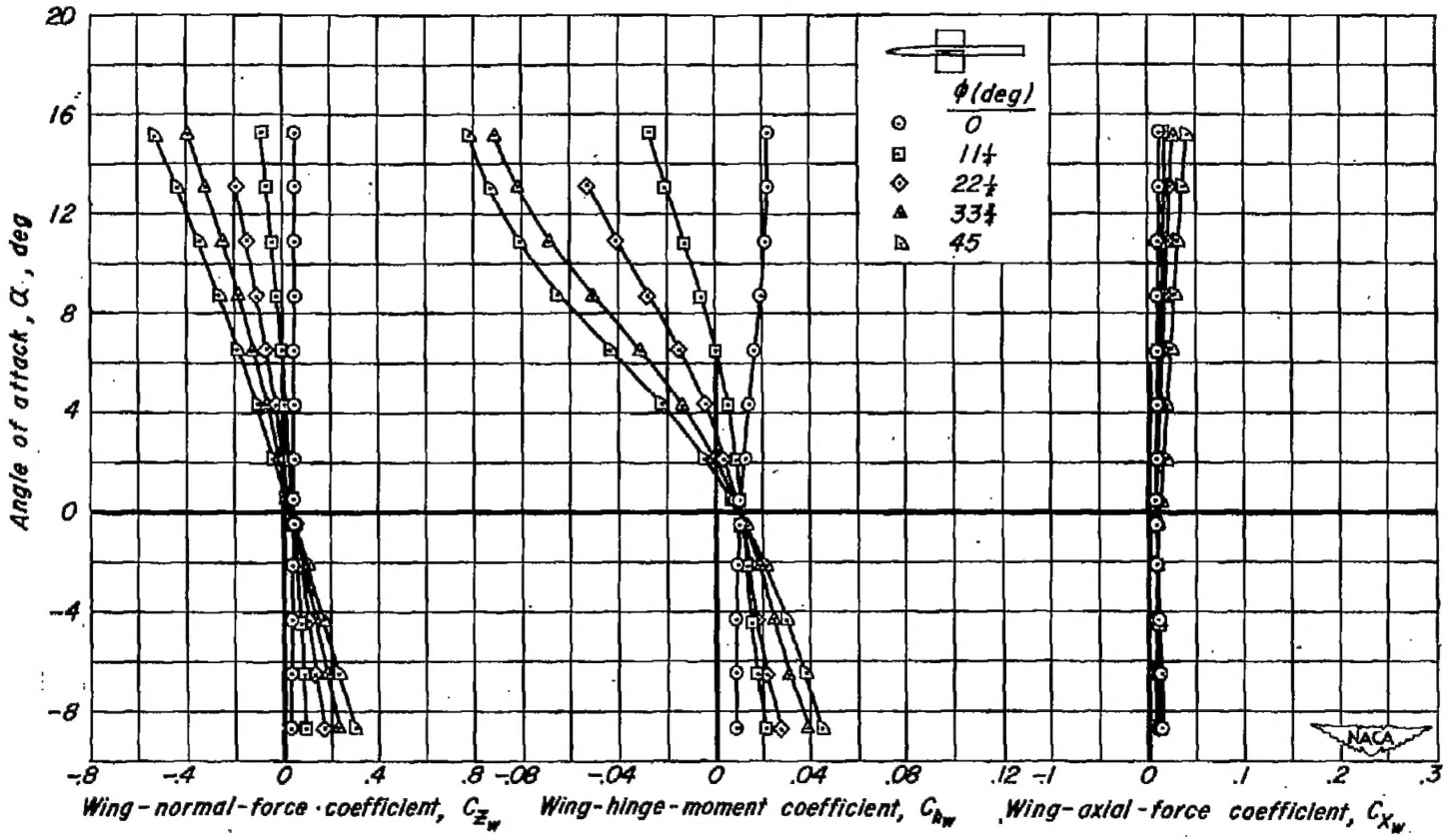

(g) Wing panel 4; Mach number, 1.4.

Figure 8.- Continued.

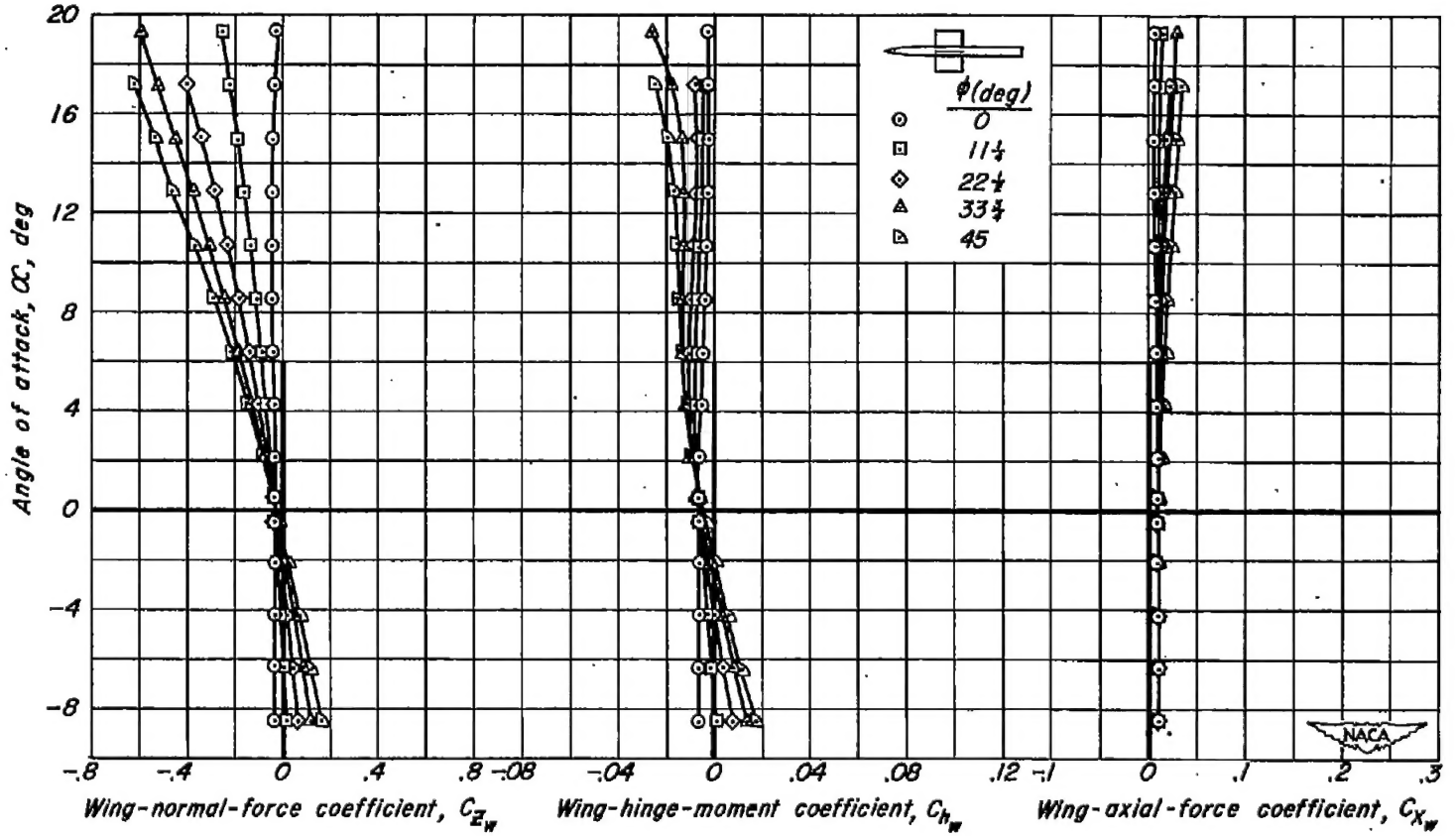

(h) Wing panel 4; Mach number, 1.9.

Figure 8.- Concluded.

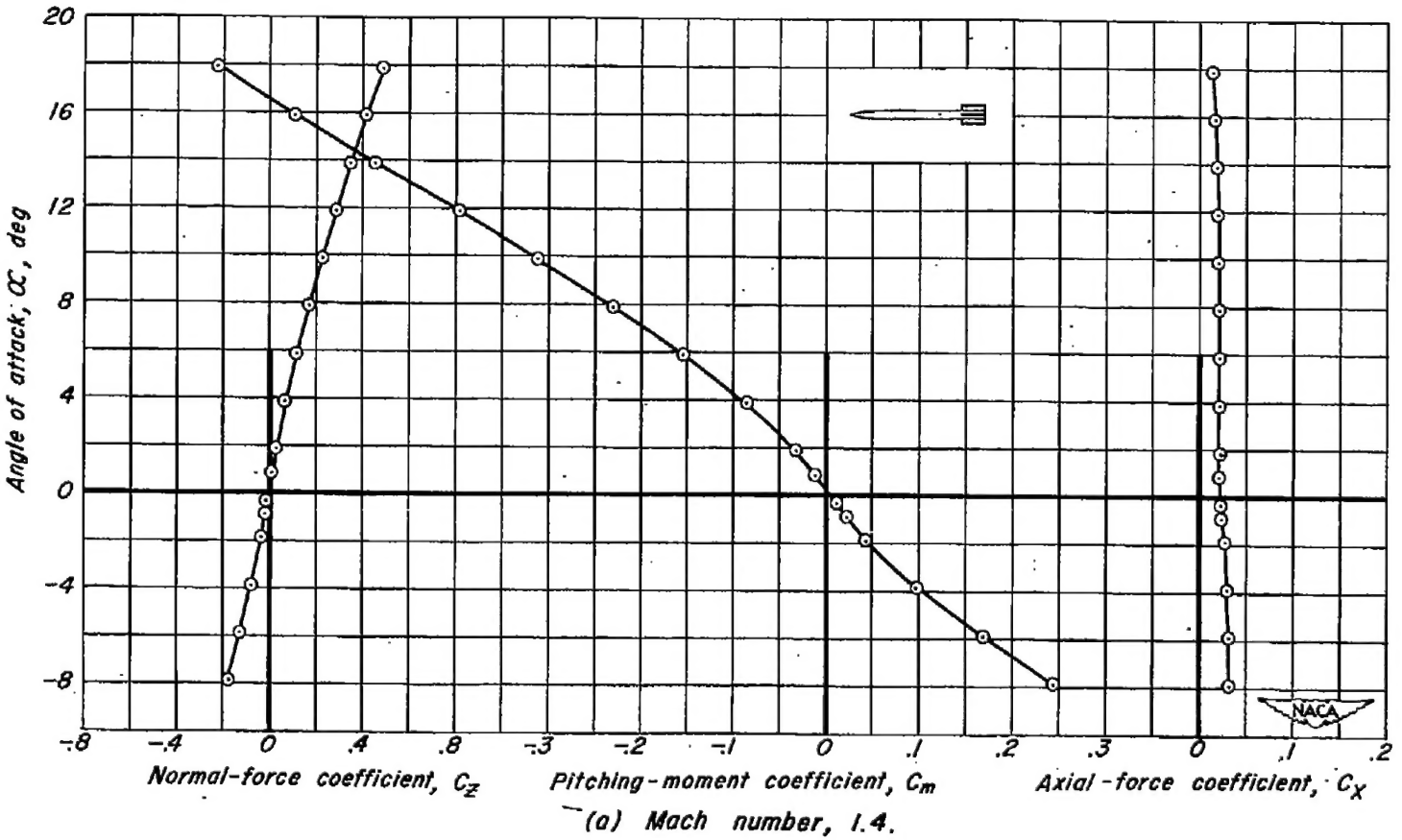

(a) Mach number, 1.4.

Figure 9.- Normal-force, pitching-moment, and axial-force characteristics of the body-tail combination at 0° bank angle.

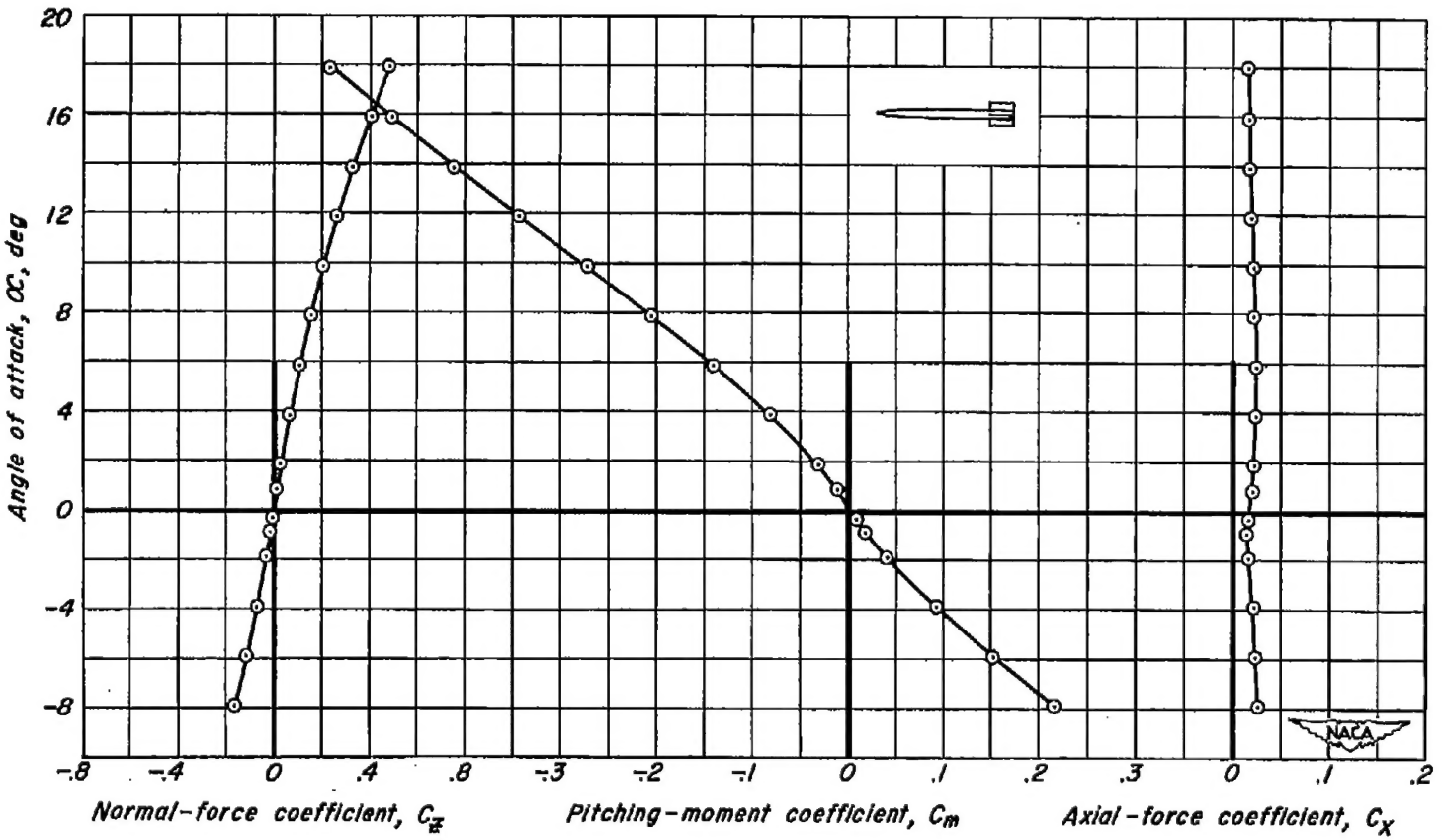

(b) Mach number, 1.9.

Figure 9.- Concluded.